GEOPHYSICAL RESEARCH LETTERS, VOL. 28, NO. 16, PAGES 3143-3146, AUGUST 15, 2001

Water vapor control at the tropopause by equatorial Kelvin waves observed over the Galápagos

M. Fujiwara,[1, 2] F. Hasebe,[3] M. Shiotani,[1, 2] N. Nishi,[4] H. Vömel,[5] and S. J. Oltmans[6]

Abstract. Soundings of frost-point hygrometers, ozonesondes, and radiosondes at San Cristóbal Island (0.9°S, 89.6°W) in September 1998 provide an observational evidence that equatorial Kelvin waves around the tropopause act as a dehydration pump for the stratosphere. During the downward-displacement phase of a Kelvin wave, dry and ozone-rich stratospheric air is transported into the upper troposphere. During the upward-displacement phase, on the other hand, higher specific-humidity air moves up in the tropopause region, but at the same time, this upward motion causes cooling of the air that limits the water vapor amount entering the stratosphere. Also, wave breaking contributes to the irreversible transport of ozone across the tropopause. Considering their omnipresence at the equatorial tropopause, we suggest that Kelvin waves may be one of the important agents for maintaining the dryness of the tropical lower stratosphere.

1. Introduction

It has been known since the 1970s that large-scale eastward-moving disturbances are prominent around the equatorial tropopause. *Madden and Julian* [1972] noted the existence of an eastward-moving disturbance at the tropopause level, in association with the 40-50-day oscillation in the troposphere, the so-called Intra-Seasonal Oscillation (ISO) or Madden-Julian Oscillation (MJO). *Parker* [1973] found the existence of marked disturbances confined around the equatorial tropopause, which have the characteristics of equatorial Kelvin waves, one of the planetary-scale eastward-moving equatorial gravity waves [e.g., *Andrews et al.,* 1987]. Before the early 1990s, however, there has been little discussion on the role of these disturbances in the variation and transport of minor constituents at the equatorial tropopause, i.e., in stratosphere-troposphere exchange (STE) (see section 1 of *Fujiwara and Takahashi* [2001]; see also section 7 of *Holton et al.* [1995], esp., p. 428). *Tsuda et al.* [1994] first suggested their role in STE by analyzing radiosonde data in Indonesia. An episode of stratospheric ozone transport into the upper troposphere associated with a breaking Kelvin wave and MJO activity below was first observed in Indonesia by *Fujiwara et al.* [1998]. A close relationship between cirrus clouds and Kelvin waves near the tropopause was first observed in the western Pacific by *Boehm and Verlinde* [2000]. Satellite water vapor measurements have shown the omnipresence of eastward-moving ISO-time-scale signals at the global equatorial tropopause [*Mote et al.,* 2000]. *Fujiwara and Takahashi* [2001] used a general circulation model incorporating a simple ozone photochemistry to show that ozone and water around the equatorial tropopause are always greatly perturbed by Kelvin waves and that there are longitudinal and seasonal differences in Kelvin wave activity.

The Soundings of Ozone and Water in the Equatorial Region/Pacific Mission (SOWER/Pacific) has been running on a campaign basis since 1998 to improve our understanding of the equatorial atmosphere by making balloon-borne measurements of ozone, water vapor, and meteorological variables at three representative stations in the equatorial Pacific, San Cristóbal Island in the Galápagos Islands (Republic of Ecuador), Kiritimati (Christmas) Island (Republic of Kiribati), and Indonesia [*Hasebe et al.,* 2001]. During the September 1998 campaign, we observed a Kelvin wave episode at San Cristóbal, in which water vapor and ozone around the tropopause showed large variations in association with this wave. In the present paper, we examine this episode in detail and discuss the role of Kelvin waves as a dehydration pump at the tropical tropopause.

2. Observation

Vertical profiles of water vapor from the middle troposphere to the middle stratosphere were measured using the NOAA/CMDL balloon-borne cryogenic frost-point hygrometers [*Vömel et al.,* 2001]. The hygrometer is launched together with an electrochemical concentration cell ozonesonde and a Vaisala RS80-15H radiosonde equipped with a Humicap-H relative humidity (RH) sensor. The radiosonde measures pressure, temperature, and RH (PTU), and is used as data transmitter. Water vapor data are obtained during the controlled descent as well as during the ascent to minimize potential contamination problems. The water vapor measurements have a typical accuracy of ~10% in mixing ratio up to the middle stratosphere. The ozone measurements have an accuracy of 5-10% in the troposphere and ~5% in the lower stratosphere. Water vapor-ozone-PTU soundings were made on September 6, 10, and 14, but the sounding on September 6 did not provide water vapor data around the tropopause. Additional soundings of ozone and PTU were made on September 4, 8, and 12. We also launched Vaisala RS80-15G radiosondes (equipped with a Humicap-A RH sensor and a Global Positioning System (GPS) antenna for the horizontal wind measurement) once or twice daily in September 1998. The RH measurement by radiosondes is available up to ~11 km for Humicap-A sensors and up to ~12-13 km for Humicap-H sensors in the tropics.

[1]Environmental Earth Science, Hokkaido University, Japan
[2]Now at RASC, Kyoto University, Japan
[3]Environmental Sciences, Ibaraki University, Japan
[4]Earth and Planetary Sciences, Kyoto University, Japan
[5]CIRES, University of Colorado, Colorado
[6]NOAA/CMDL, Colorado

Paper number 2001GL013310.
0094-8276/01/2001GL013310$05.00

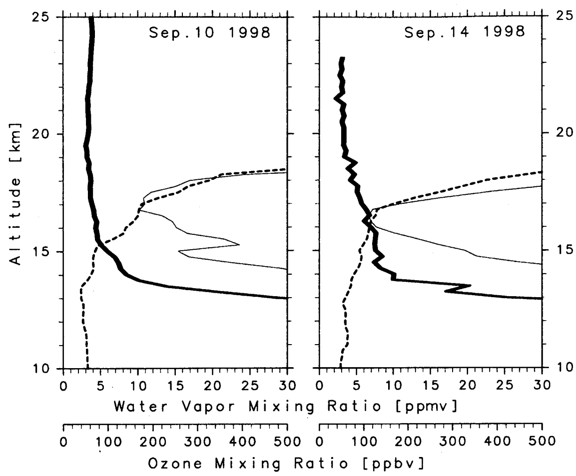

Figure 1. Profiles of water vapor mixing ratio (thick curves), saturation water vapor mixing ratio calculated from ambient temperature using the Goff-Gratch formulation (thin curves), and ozone mixing ratio (dashed curves) at San Cristóbal on September 10 and 14, 1998. The plotted data are 250 m averages. For water vapor and temperature, both ascending and descending data are averaged, whereas for ozone, only ascending data are used.

3. Results and Discussion

Figure 1 shows the results of the hygrometer soundings on September 10 and 14. The water vapor mixing ratio above 18 km up to the middle stratosphere was 3-4 ppmv in both soundings, but water vapor, ozone, and saturation mixing ratio show large changes in the tropopause region (14-18 km) during this 4-day period. On September 10, dry stratospheric air extended down to 15.25 km (5.18 ppmv), and ozone concentrations were enhanced in the tropopause region (211 ppbv at 17.25 km (tropopause)). The tropopause region was unsaturated due to high ambient temperature and low frost-point temperature. These features are consistent with adiabatic downward motion occurring around the tropopause. On September 14, on the other hand, the tropopause region was relatively wet (6-10 ppmv at 14-16.5 km) and cold, hence nearly saturated at 16-17 km, and the ozone concentration was lower (127 ppbv) at the tropopause (16.5 km).

Figure 2 shows all ozone profiles during the campaign. On September 4 and 6, the tropopause nearly corresponded to the "ozonopause" which is the boundary between the region with tropospheric low ozone concentrations and that with stratospheric high ozone concentrations. Here, we use 125 ppbv as the ozonopause value. On September 8, the tropopause was at its lowest altitude, ~15 km. While the ozonopause remained around 16 km during September 8-12, the tropopause moved upward from ~15 to 17-17.5 km, leaving a significant amount of stratospheric ozone in the upper troposphere. On September 14, the ozonopause and tropopause were located at nearly the same altitude again. The characteristics of ozone and tropopause variations resemble the case observed by *Fujiwara et al.* [1998] (see their Figures 2 and 4).

Figure 3 shows the time-altitude distributions of ozone, temperature, potential temperature, and zonal wind at San Cristóbal in September 1998. We can see a downward motion of ozone in the tropopause region, from ~18 km on September 4 to ~14 km on September 14. While isolines for mixing ratios greater than 125 ppbv recovered by September 14, the 75-ppbv isoline continued to move downward to as low as 14 km. Figures 3(b)-(d) utilize radiosonde data as well to investigate the disturbance in detail. Before September 8, the tropopause was colder and gradually moving downward. After the tropopause jump around September 8-9, the tropopause was again moving downward and getting colder. The temperature change associated with this disturbance was ~7 K at 16 km (from 194 K on September 7 to 201 K on September 10). The potential temperature plot indicates that before September 8, the isentropes near and just above the tropopause were moving downward and that after the tropopause jump, their downward motion continued and extended into the upper troposphere. We can see a downward-motion line from 17.5 km on September 2 to 14 km on September 15, although the motion of individual isentropes is smaller. At the same time, a zonal wind oscillation was observed in the 12-19-km region, with the period ($2\pi\omega^{-1}$, where ω is the frequency) of ~18 days (ex., from September 2 to 20, at 16 km). The downward-motion line for isentropes nearly corresponded to the zero zonal wind line, which indicates that the vertical phase speed of this disturbance, $c^{(z)}$, was -3.1×10^{-3} m s^{-1}. The background zonal wind in September 1998 was nearly zero at 15-19 km, and the amplitude of this disturbance, U, was ~15 m s^{-1} at 16 km. There was no substantial meridional-wind component (not shown) corresponding to this zonal wind oscillation. These meteorological characteristics again resemble the case observed by *Fujiwara et al.* [1998] (see their Figures 4 and 5 and Plate 1). If we focus only on the tropopause level, the water vapor-ozone sounding on September 10 measured the downward-displacement phase of this disturbance, and the sounding on September 14 measured the neutral or upward-displacement phase of this disturbance.

The equatorial longitude-time distribution of temperature

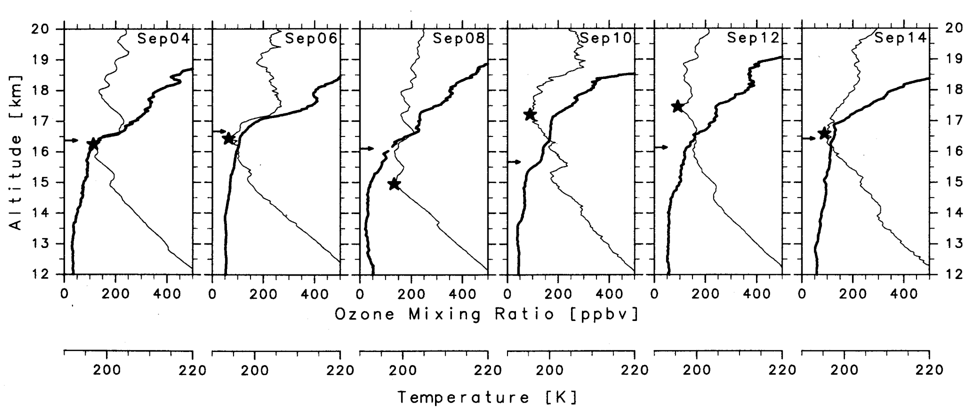

Figure 2. Profiles of ozone (thick) and temperature (thin) from 12 to 20 km on September 4, 6, 8, 10, 12, and 14, 1998 at San Cristóbal. Stars indicate the location of the tropopause defined by the temperature minimum. Horizontal arrows indicate the location of the ozonopause defined by 125-ppbv ozone concentration.

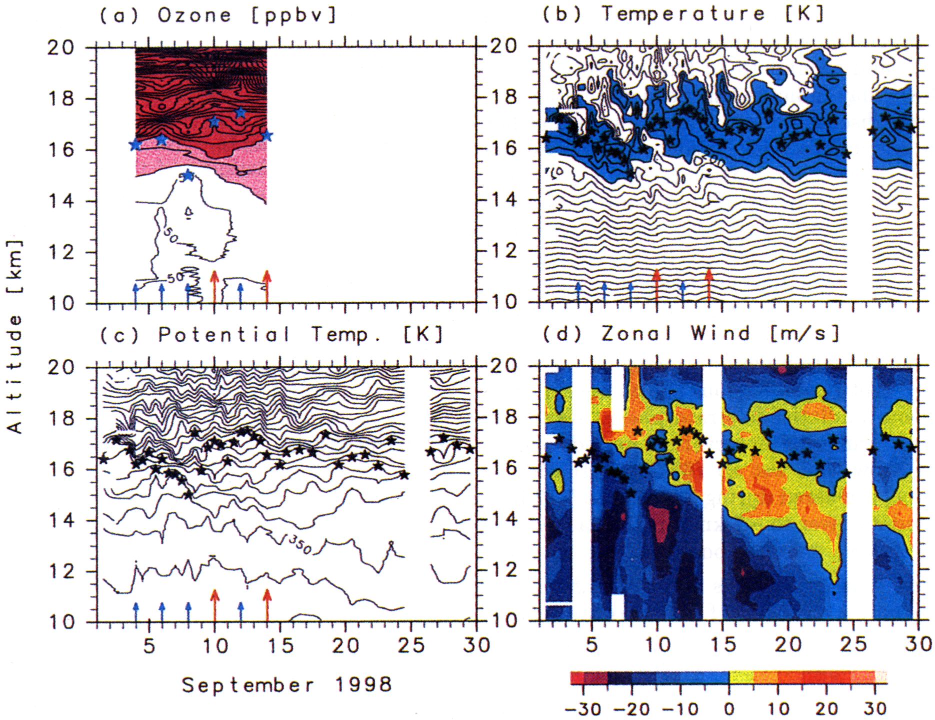

Figure 3. Time-altitude distributions of (a) ozone (25-ppbv interval, pink for 75-125 ppbv, red for more than 125 ppbv), (b) temperature (2-K interval, blue for less than 200 K), (c) potential temperature (5-K interval), and (d) zonal wind from 10 to 20 km at San Cristóbal in September 1998. Vertical resolution here is set to 50 m. Stars indicate the location of the tropopause. Blue and red arrows in (a)-(c) indicate ozonesonde soundings and hygrometer-ozonesonde soundings, respectively.

at 100 hPa (European Centre for Medium-Range Weather Forecast (ECMWF) global analysis data) shows the horizontal extent and motion of this disturbance (Figure 4). The eastward-moving warm anomaly (slanted line) corresponds to the warm, descending anomaly observed at San Cristóbal around September 10. This eastward-moving signal attains a large amplitude over the western Pacific in late August, moves eastward with a zonal phase speed, $c^{(x)}$, of $\sim$14 m s^{-1}, and becomes weak over South America in the middle of September. Figure 4 also shows that eastward-moving signals over the eastern Pacific and South America are sporadic and that those over the Indian Ocean are regularly present with larger amplitudes [cf., *Fujiwara and Takahashi*, 2001]. It should be noted that in the ECMWF zonal wind data (not shown), the eastward-moving signal relevant to the observation at San Cristóbal is very weak.

The characteristic values for the disturbance ($2\pi\omega^{-1}$, $c^{(x)}$, and $c^{(z)}$) estimated above reasonably satisfy the dispersion relation for equatorial Kelvin waves (see section 3 of *Fujiwara et al.* [1998]). Note that the buoyancy (or Brünt-Väisälä) frequency, N, at 16 km is on average $\sim$1.8 $\times 10^{-2}$ s^{-1} with a large positive vertical gradient in the tropopause region, from $\sim$0.8 $\times 10^{-2}$ s^{-1} at 10-13 km to $\sim$2.3 $\times 10^{-2}$ s^{-1} at 17 km and above. Thus, the disturbance observed at San Cristóbal in September 1998 can be identified as an equatorial Kelvin wave because: It had a zonal-wind component but no meridional-wind component; it propagated eastward; its warm anomaly appeared at the zero zonal wind phase with the eastward-wind shear (note that the background zonal wind was zero); and its characteristic parameters reasonably satisfied the dispersion relation for equatorial Kelvin waves. The maximum vertical displacement by this wave can be estimated from $2U/N$ (see section 4.1 of *Fujiwara et al.* [1998]) to be $\sim$1.7 km for $N = 1.8 \times 10^{-2}$ s^{-1}. The downward motion of the ozone isolines and isentropes is in reasonable agreement with this estimate. Furthermore, the zonal wind amplitude, U was comparable to the (intrinsic) zonal phase speed of the wave, $c^{(x)}$, so that breaking of the wave, i.e., vertical mixing is expected at least at the maximum eastward-wind phase of the wave (see section 4.2 of *Fujiwara et al.* [1998]). The vertical extent of this mixing region should be less than $\sim$2.4 km, half of the vertical

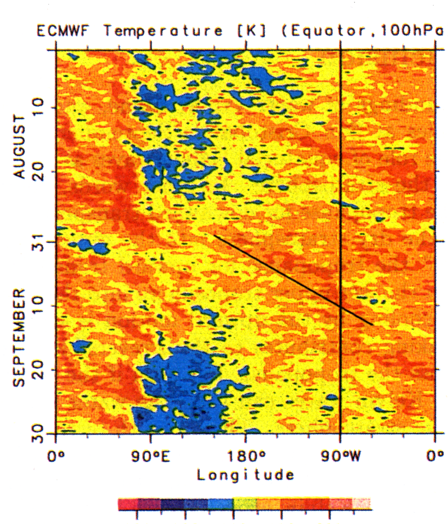

Figure 4. Longitude-time distribution of temperature at 100 hPa along the equator from the ECMWF global analysis data (twice daily, 2.5°×2.5°). The vertical line indicates the location of San Cristóbal, and the slanted line indicates the warm anomaly moving eastward and passing over San Cristóbal around September 10.

wavelength $((2\pi\omega^{-1})c^{(z)}/2)$. Nearly constant ozone concentrations around 18 km on September 6-8, around 17 km on September 8-12, and around 15-16 km on September 14 (Figures 2 and 3(a)) may indicate this vertical mixing.

Finally, we briefly discuss potential contributions of horizontal advection and convection. Similar to the estimation of the vertical displacement, the maximum zonal displacement by this wave can be estimated from $2U/\omega$ to be $\sim 7.4\times 10^3$ km. We also made trajectory calculations with the ECMWF data. Seven-day isentropic backward trajectories from the tropopause region at San Cristóbal on September 10 showed that the air was mostly influenced by transport from tropical South America and the Atlantic within 0-10°N. During the observation period, the region was sometimes influenced by subtropical air, but the enhanced ozone never originated from midlatitude stratosphere. As for the convective activity during the observation period, the radiosonde RH data show that wet air (60-90% RH with respect to liquid water) appeared during September 5-12 from the top of the boundary layer to ~7 km but that a dry layer (<30% and often <10%) existed above the wet air mass, from ~7 to ~11 km. Thus, there was no direct influence of cumulus convection on the variation of minor constituents in the tropopause region. Satellite infrared cloud images confirm that there was no significant cloud activity along the equator in the central and eastern Pacific during the period, although some active convection was present around 10°N in the eastern Pacific.

These observational results suggest that Kelvin waves around the tropopause include the following processes that cause stratosphere-troposphere exchange and maintain the dryness of the tropical lower stratosphere. During the downward-displacement phase of a Kelvin wave (September 10 at San Cristóbal), dry and ozone-rich stratospheric air is transported into the upper troposphere. During the upward-displacement phase (September 14, at the tropopause level), higher specific-humidity air moves up, but this upward motion causes adiabatic cooling, which at the same time limits the water vapor amount entering the stratosphere. When the wave amplitude becomes large enough to meet the breaking condition, irreversible mixing occurs at the maximum eastward-wind phase, resulting in net transport of ozone across the tropopause.

4. Conclusion

The soundings of water vapor, ozone, and meteorological variables at San Cristóbal in September 1998 demonstrated the role of equatorial Kelvin waves as a dehydration pump for the stratosphere. In other words, Kelvin waves "open" the tropopause for downward transport of water vapor from the dry stratosphere into the upper troposphere, but "close" the tropopause for upward transport of water vapor from the wet upper troposphere into the stratosphere when the cooling by the upward motion is strong enough. Wave breaking contributes to the irreversible transport of ozone across the tropopause, but even if the breaking does not occur, Kelvin waves can limit the water vapor amount entering the stratosphere. The strength of the cooling due to the upward motion by the wave is the critical factor. We also see that shorter-period, smaller-amplitude waves were enbedded in the Kelvin wave (Figure 3(d), for example), which might also play a role in the dehydration as suggested by *Potter and Holton* [1995]. The present study highlights the role of Kelvin waves in tropical stratosphere-troposphere exchange. Intensive, coordinated observation campaigns are needed to further investigate a possible dynamical-radiative-physical-chemical coupling in association with these large-scale tropopause-level waves.

Acknowledgments. We thank M. Agama, J. Cornejo, F. Paredes, and H. Enriquez of the Instituto Nacionál de Meteorología e Hidrología (INAMHI), Ecuador for assisting us in making the soundings at San Cristóbal Island. The observations were financially supported by Sumitomo Foundation, Monbusho International Scientific Research Program, and Asahi Breweries Foundation. M.F. was supported by research fellowships of the Japan Society for the Promotion of Science for Young Scientists. Comments on the manuscript by reviewers were greatly appreciated. The figures were produced with the GFD-DENNOU Library.

References

Andrews, D. G., J. R. Holton, and C. B. Leovy, *Middle Atmosphere Dynamics,* 489 pp., Academic, San Diego, Calif., 1987.

Boehm, M. T., and J. Verlinde, Stratospheric influence on upper tropospheric tropical cirrus, *Geophys. Res. Lett., 27,* 3209-3212, 2000.

Fujiwara, M., K. Kita, and T. Ogawa, Stratosphere-troposphere exchange of ozone associated with the equatorial Kelvin wave as observed with ozonesondes and rawinsondes, *J. Geophys. Res., 103,* 19,173-19,182, 1998.

Fujiwara, M., and M. Takahashi, The role of the equatorial Kelvin wave in stratosphere-troposphere exchange in a general circulation model, *J. Geophys. Res.*, in press, 2001.

Hasebe, F., et al., Initial results from SOWER/Pacific 1998-2000 campaigns, *Proceedings of the 2nd SPARC General Assembly* (printed in CD-ROM), 2001.

Holton, J. R., P. H. Haynes, M. E. McIntyre, A. R. Douglass, R. B. Rood, and L. Pfister, Stratosphere-troposphere exchange, *Rev. Geophys., 33,4,* 403-439, 1995.

Madden, R. A., and P. R. Julian, Description of global-scale circulation cells in the tropics with a 40-50 day period, *J. Atmos. Sci., 29,* 1109-1123, 1972.

Mote, P. W., H. L. Clark, T. J. Dunkerton, R. S. Harwood, and H. C. Pumphrey, Intraseasonal variations of water vapor in the tropical upper troposphere and tropopause region, *J. Geophys. Res., 105,* 17,457-17,470, 2000.

Parker, D. E., Equatorial Kelvin waves at 100 millibars, *Q. J. R. Meteorol. Soc., 99,* 116-129, 1973.

Potter, B. E., and J. R. Holton, The role of monsoon convection in the dehydration of the lower tropical stratosphere, *J. Atmos. Sci., 52,* 1034-1050, 1995.

Tsuda, T., Y. Murayama, H. Wiryosumarto, S. W. B. Harijono, and S. Kato, Radiosonde observations of equatorial atmosphere dynamics over Indonesia, 1, Equatorial waves and diurnal tides, *J. Geophys. Res., 99,* 10,491-10,505, 1994.

Vömel, H., et al., Balloon-borne observations of water vapor and ozone in the tropical upper troposphere and lower stratosphere, *J. Geophys. Res.*, submitted, 2001.

M. Fujiwara, and M. Shiotani, Radio Science Center for Space and Atmosphere (RASC), Kyoto University, Kyoto 611-0011, Japan. (e-mail: fuji@kurasc.kyoto-u.ac.jp)

F. Hasebe, Department of Environmental Sciences, Ibaraki University, Ibaraki 310-8512, Japan.

N. Nishi, Department of Earth and Planetary Sciences, Kyoto University, Kyoto 606-8502, Japan.

H. Vömel, CIRES, University of Colorado, Boulder, CO 80309-216.

S. J. Oltmans, NOAA/CMDL, Boulder, CO 80305.

(Received April 17, 2001; revised June 6, 2001; accepted June 14, 2001.)